SUPPORTING INFORMATION PARAGRAPH

Chamber pressure, total number of drops, and average drop diameter vs. time

Past initial nucleation, the drop nanoparticle surface coverage can increase via two mechanisms. In the first mechanism, the nanoparticles can migrate to the drop surface via liquid vapor meniscus as the drop expands over additional nanoparticles by direct vapor condensation. In the second mechanism, the nanoparticles can move from below to side or top of the drops during a coalescence event between two drops. In general the dominating drop growth mechanism can be systematically determined by evaluating the average drop diameter, <d>, as a function of time.[1-4] Typically <d> grows according to the power law $\langle d \rangle \sim t^{\alpha}$, where $\alpha=1/3$ for individual droplet growth via direct vapor condensation on any surface and $\alpha=1$ or $\alpha=0$ for coalescence dominated growth on patterned hydrophobic[5-8] or superhydrophobic surfaces,[9-10] respectively. We manually measured the diameter, d, defined as four times the area divided by the perimeter of the drops[11] for every other image in the sequence shown in Figure 2 a. After the raw images were processed with Enhanced Local Contrast (CLAHE) function, the drops were manually highlighted using Segmentation Editor, binarized, separated using Watershed algorithm, and analyzed using the Analyze Particles function in the FIJI image analysis software.[12] As shown in Figure 1, <d> increases with time at two distinct rates. Specifically, <d> is relatively stagnant for the first 8 seconds and increases approximate linearly afterwards. However, the increase in <d> growth rate cannot be used to support growth mechanism switch from direct condensation to coalescence because it was forced by ESEM chamber pressure increase (also plotted on Figure 1). In typical ESEM experiments, the rate of condensation is controlled by cooling the substrate and carefully increasing the chamber pressure past the saturation point. To capture the microscale details of the process without prior sample damage due to beam exposure (see Methods sections) the pressure has to be carefully increased in small steps with an initially blanked beam. Insufficient increase in pressure will trigger but not sustain continued condensation. This is illustrated in Figure 1, with <d> remaining nearly constant around 2 µm during pressure increase from ~675 Pa to ~750 Pa. Increase in pressure past 750 Pa triggers further growth of the drops. In summary, because the ESEM experiments are performed in pressure varying mode[13-14] the drops do not grow under steady state conditions and fitting the growth rate law is not appropriate method of determining the drop growth mechanism.

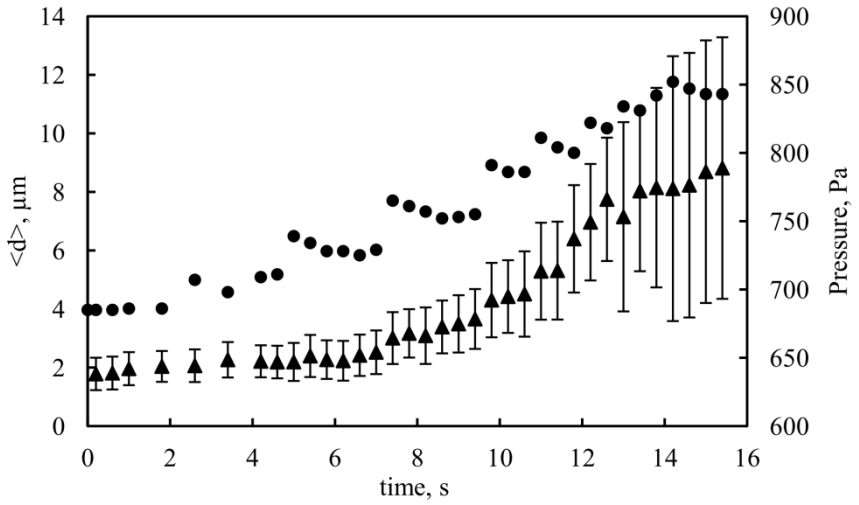

Figure 1. Average drop/liquid marble diameter, <d>, and ESEM chamber pressure vs. time corresponding to initial condensation process shown in Figure 2 of the paper. The error bars correspond to one standard deviation of the drop size distribution.

However, drop growth via coalescence is likely the dominating growth mechanism because of the drastic decrease in the total number of drops from ~150 to ~20 during the 6 s to 18 s time range in process (see Figure 2 below). As pointed out by the white arrows in Figure 2 in the paper, visible nanoparticle coverage of the droplets begins within the same time period. Lastly, we have also repeated the experiment under ambient conditions and

imaged it optically but because the nanoparticles are optically transparent judgment about their location on the drops could not be made.

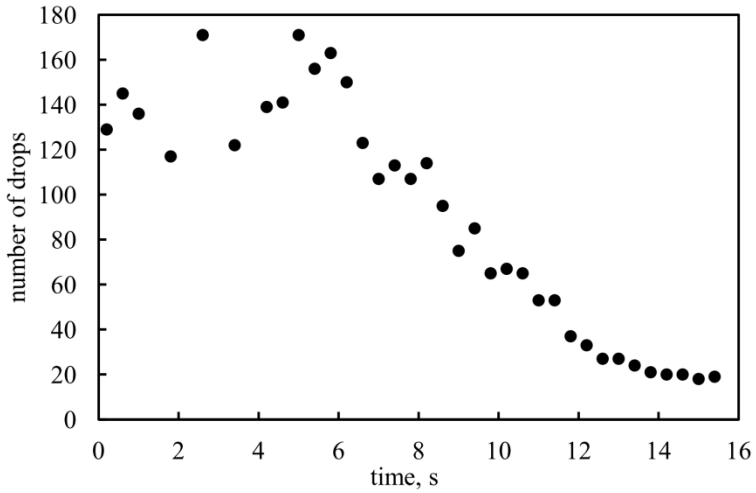

Figure 2. Total number of drops vs. time corresponding to initial condensation process shown in Figure 2 of the paper.

FIB cross-sectioning and imaging procedure

FIB cutting was performed using an FEI Nova 600 DualBeam.[†] To avoid shape distortion due to direct ion beam exposure and indirect effects such as material redeposition, the fabricated structures were coated with platinum using Focused Ion Beam Induced Deposition (FIBID) using $C_9H_{16}Pt$ gas precursor, an ion beam energy of 30 keV, an ion current of 210 pA, and a dwell time of 200 ns per pixel. The structure cross sections are obtained by FIB milling about 3 µm deep trenches at an ion current of 2.6 nA and polishing of the surfaces at a lower current of 48 pA, with both milling steps performed at an ion beam energy of 30 keV. All structures are imaged at 52° tilt using an electron beam current of 0.4 nA and an electron beam energy of 5 keV. The captured images were analyzed using the ImageJ analysis software package.[15] All reported thickness values are averages of six measurements with associated standard error.

TEM imaging and particle size distribution measurement

To characterize the nanoparticle morphology, loose nanoparticle powder was suspended in ethanol, ultrasonicated for 5 minutes, and dropcasted onto a holey carbon substrate film mounted on a 3 mm copper TEM grid. Full-field TEM images were acquired at 300 keV using an FEI CM300FEG transmission electron microscope equipped with a Gatan imaging energy filter (GIF2000). TEM micrographs were obtained using a post-prism Gatan multiscan CCD camera, with the GIF operated in both unfiltered mode and elastic only mode with an energy selecting slit width of 10 eV. The approximate magnification of the imaging system was determined using a carbon diffraction grating replica with 2160 lines/mm.

Optical imaging set up

Figure 3. Images of the optical set up used to study liquid marble formation during condensation.

Contact Angle Measurement on superhydrophobic surface with the nanoparticle film

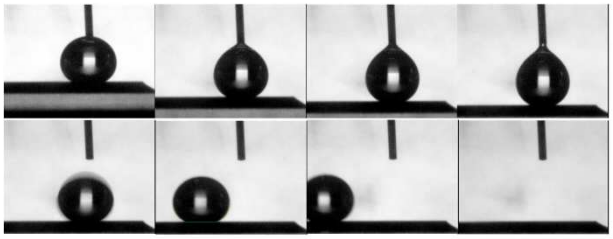

Figure 4. Images demonstrating droplets bouncing and rolling off the superhydrophobic surface covered with the nanoparticles.

† Certain commercial equipment, instruments, and materials are identified in this publication to adequately specify the experimental procedure. Such identification in no way implies approval, recommendation, or endorsement by NIST, nor does it imply that the equipment, instruments, or materials identified are necessarily the best available for the purpose.

References:

1. Beysens, D.; Knobler, C. M., Growth of Breath Figures. *Phys. Rev. Lett.* **1986,** *57* (12), 1433-1436.
2. Viovy, J. L.; Beysens, D.; Knobler, C. M., Scaling Description for the Growth of Condensation Patterns on Surfaces. *Physical Review A* **1988,** *37* (12), 4965-4970.
3. Beysens, D.; Knobler, C. M.; Schaffar, H., Scaling in the Growth of Aggregates on a Surface. *Phys. Rev. B* **1990,** *41* (14), 9814-9818.
4. Beysens, D., Dew Nucleation and Growth. *Comp. Rend. Phys.* **2006,** *7* (9-10), 1082-1100.
5. Narhe, R. D.; Beysens, D. A., Nucleation and Growth on a Superhydrophobic Grooved Surface. *Phys. Rev. Lett.* **2004,** *93* (7), 076103.
6. Narhe, R. D.; Beysens, D. A., Water Condensation on a Super-Hydrophobic Spike Surface. *Europhys. Lett.* **2006,** *75* (1), 98-104.
7. Narhe, R. D.; Beysens, D. A., Growth Dynamics of Water Drops on a Square-Pattern Rough Hydrophobic Surface. *Langmuir* **2007,** *23* (12), 6486-6489.
8. Narhe, R. D.; González-Viñas, W.; Beysens, D. A., Water Condensation on Zinc Surfaces Treated by Chemical Bath Deposition. *Appl. Surf. Sci.* **2011,** *256* (16), 4930-4933.
9. Boreyko, J. B.; Chen, C. H., Self-Propelled Dropwise Condensate on Superhydrophobic Surfaces. *Phys. Rev. Lett.* **2009,** *103* (18), 184501-1-184501-4.

10. Chen, X.; Wu, J.; Ma, R.; Hua, M.; Koratkar, N.; Yao, S.; Wang, Z., Nanograssed Micropyramidal Architectures for Continuous Dropwise Condensation. *Adv. Funct. Mater.* **2011,** *DOI: 10.1002/adfm.201101302*.
11. Rykaczewski, K.; Scott, J. H. J.; Fedorov, A. G., Electron Beam Heating Effects During Environmental Scanning Electron Microscopy Imaging of Water Condensation on Superhydrophobic Surfaces. *Appl. Phys. Lett.* **2011,** *98* (9), 093106-1-093106-3.
12. *Fiji*, http://fiji.sc.
13. Anand, S.; Son, S. Y., Sub-Micrometer Dropwise Condensation under Superheated and Rarefied Vapor Condition. *Langmuir* **2010,** *26* (22), 17100-17110.
14. Rykaczewski, K.; Scott, J. H. J.; Rajauria, S.; Chinn, J.; Chinn, A. M.; Jones, W., Three Dimensional Aspects of Droplet Coalescence During Dropwise Condensation on Superhydrophobic Surfaces. *Soft Matter* **2011,** *7*, 8749-8752.
15. Rasband, W. S. Imagej. http://rsb.info.nih.gov/ij/.